

PARAMETRIC OPTIMIZATION AND EXPERIMENTAL ANALYSIS OF WIRE EDM RESPONSES IN A GEAR CUTTING PROCESS

K.D. Mohapatra¹, S.K. Sahoo²

¹Ph. D Research Scholar, ²Professor

Department of Mechanical Engineering, National Institute of Technology, Rourkela, 769008

Abstract: Wire EDM is a non-traditional machining operation in which complicated profiles are cut by the help of a wire by the application of heat produced from the electrical sparks. Gear cutting is a challenging task in which small teeth are cut by the help of wire for the manufacturing of gears to meet the growing demand. The objective of the present work is to minimise the error present in the gears by optimising the input parameters to get the optimum value. The proposed work deals with the analysis and optimisation of response parameters, i.e., single pitch error and material removal rate of wire electric discharge machined spur gears made of copper material. The values of single pitch error and MRR of the gear obtained by these experiments were optimised and a loss function is generated by optimising the single pitch error and MRR. Microstructural analysis has been carried out at the optimized settings to know the surface defects of both material and the wire electrode. Numerical modelling using ANSYS has been carried out to know the temperature of the workpiece. The loss function is investigated and the optimum settings obtained can be applied for future findings.

Keywords: Gear, Wire EDM, Single pitch error, Material removal rate, Spur gears

I. INTRODUCTION

Wire electric discharge machining (WEDM) is a non-conventional machining process for cutting of complex and hard materials that are difficult to manufacture by other non-conventional machining process. A good precision with accuracy and a better surface finish is obtained by this process. It has the ability to cut the conductive materials requiring no further polishing or finishing. In wire EDM, pulse discharge occurs in a small gap between the work-piece and the electrodes and removes the unwanted material from the parent material by melting and vaporizing the metal in presence of dielectric fluid. In the year 1960, the first wire cut type machine emerges for the purpose of making tools and dies from the hardened steels. In 1967, David H. Dulebohn's group built a Wire cut EDM machine which was the first available commercial NC machine in the USSR at Andrew Engineering Company for milling and grinding operations [1]. The tool electrode is basically a wire made of brass supplied from the spool and the diameter of the wire ranges from 0.1 mm to 0.3 mm [2]. Proper codes should be given to the wire EDM machine to cut very fine and delicate shapes of materials by controlling the axis movement. The two guides i.e. the upper guide and lower guide moves independently and is controlled by the CNC machine. As

there is no direct contact between the tool and the work-piece, material (generally conductive) of any hardness can be machined as long as the wire is electrically conductive [3]. The material removal occurs by continuous spark discharges between the tool and the work-piece. Many sparks occur during cutting at one time which ranges from 1/1000000 of a second or less. The temperatures are so high that it is enough to melt the metal in the area of electrical discharges [4]. The wire once used cannot be reused again, and is collected at the bottom of the tank [5]. Flushing is an important parameter in wire EDM and it uses distilled water as dielectric. Water flows from both the upper and lower guides, and the flow of water can also be controlled from the machine. The importance of flushing is it acts as a coolant and flushes away the cut debris from the metal surface. Wire EDM provides a good surface finishing operation with no burrs. In order to obtain a good results and better accuracies, the wire EDM input parameters should be set properly. Wire EDM has a wide range of applications in many industries like tool and die making, computer and electronics, automobile, aerospace and nuclear tool etc. It becomes a preferred choice for manufacturing the miniaturized components including gears.

Gears are the key elements to the manufacturing processes. Gears having external diameter less than 10 mm are known as miniature gears whereas gears having external diameter more than 10 mm are known as meso gears. A large number of gears mesh together with other gears to produce torque. So in order to avoid interference and inaccuracy in the mating of the gear tooth while meshing, the teeth's of the gear should be machined properly. WEDM can be a suitable option in this regard as it produces good surface finish and accuracy with no burr. Copper gears find its application in various transportation oils such as diesel, petroleum, semiconductor industries, lubricant oils, clocks, radiators, aerospace, printing, papermaking, mining industries, electric motors, trucks and air brakes

II. LITERATURE REVIEW

Wire electric discharge machining (WEDM) has become a preferred choice for manufacturing the miniaturized components. Many researchers have analysed the WEDM process applied to different materials at different working conditions and reported their experimental findings. Some of the worth mentioning works include the use of a combination of neural network and simulated annealing by Tarnq et al. [6], Taguchi's L18 orthogonal array by Liao et al. [7], a combination of grey relational analysis and Taguchi's L18 orthogonal array by Huang and Liao [8], Taguchi's L16

orthogonal array by Ramakrishna and Karunamoorthy [9] and a combination of response surface methodology and desirability analysis by Kanlayasiri and Jattakul [10]. Gupta and Neelesh Jain [11] emphasized on micro geometry of miniature gears produced by Wire EDM. They optimized the total profile deviation and accumulated pitch deviation of miniature spur gears made of brass. NihatGogun and Tosun[12] experiment the kerfs and material removal rate in wire electrical discharge machining based on Taguchi method. They investigate the effects and optimization of machining parameters on the kerf (cutting width) and material removal rate (MRR) in wire electrical discharge machining operations.

From the past literature it has been found that less work has been carried out on optimization of gear errors and surface integrity of the gears by wire EDM process. So the objective of the present work is to analyse and investigate the single pitch error and MRR of the gear made of copper and to find an optimized settings for which the gear can be manufactured easily without fail.

III. EXPERIMENTAL DETAILS AND METHODS

The present work deals with the manufacturing of gears from a 3 mm rectangular copper plate of 10 mm in length and 5 mm width of an ECOCUT® CNC wire EDM machine. The tool electrode used is brass wire and the diameter of the wire is 0.25 mm. De-ionized water is used as the dielectric for this experiment. Table 1 and Table 2 show the composition of tool wire (Brass) and the work-piece material (Copper). Fig. 1 shows the schematic diagram of a Wire EDM process cutting a gear.

TABLE I. COMPOSITION OF WEDM BRASS (CUZN37) WIRE

Cu	Zn	Sn	P	Fe	Al	Ni	Diameter	Tensile strength
63%	36.5%	0.12%	0.02%	0.01%	0.05%	0.27%	0.25	900 N/mm ²

TABLE II. COMPOSITION OF COPPER WORKPIECE

Cu+Ag	Pb	S	Bi	Fe	As	Sb
99.90%	0.005%	0.005%	0.001%	0.005%	0.002%	0.002%

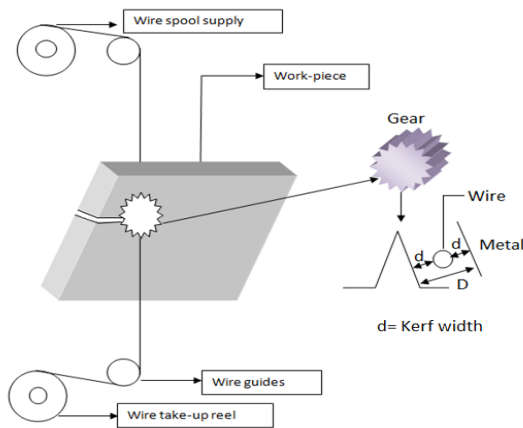


Fig. 1.Schematic diagram of wire EDM gear cutting process. In this experiment four input parameters i.e. Pulse on time (T_{on}), Pulse off time (T_{off}), Wire feed rate (W_f) and Wire tension (W_t) were taken at four different levels. The values and ranges of these parameters are chosen within the machine

constraints are shown in Table 3. The fixed and variable parameters used in the experimentation are shown in Table 4. The copper plate is machined by the help of wire EDM to produce gear having sixteen numbers of teeth as shown in Fig. 2. For the calculation of single pitch error, a minimum of two teeth's are required. So two gears are formed with each having sixteen numbers of teeth were machined by WEDM.

TABLE III. INPUT PARAMETERS AND RANGES USED IN THE EXPERIMENTATION

Input Parameter	Symbol	Unit	Levels			
			I	II	III	IV
Pulse on time	T_{on}	μs	110	112	114	116
Pulse off time	T_{off}	μs	50	52	54	56
Wire feed rate	W_f	m/min	3	4	5	6
Wire tension	W_t	Kg-f	6	7	8	9

TABLE IV. FIXED PARAMETERS AND GEAR SPECIFICATIONS USED IN THE EXPERIMENT

Constant Parameters		Gear specifications	
Wire type	Brass	Material	Copper
Wire Diameter	0.25mm	Profile	Involute
Servo Voltage (S_v)	10V	Pressure angle	20°
Peak Current (I)	1A	Number of teeth	32
Dielectric	Distilled water	Tooth Width	4.90 mm
Water Pressure (W_p)	1kg/cm ²	Base diameter	46.98 mm
Peak Voltage (V_p)	11V	Pitch circle Diameter	50 mm

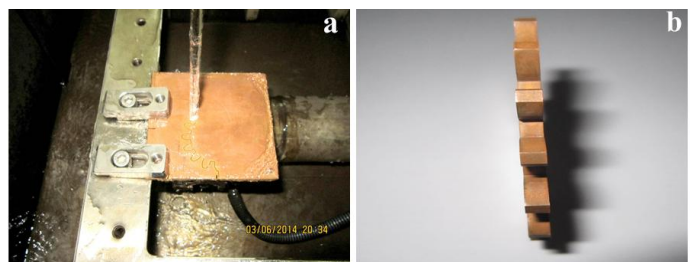


Fig. 2.Machining of copper plate by wire EDM having sixteen numbers of teeth.

The meso spur gear is obtained by using ELCAM software after inputting various data's like Pressure angle (20°), Pitch circle diameter (50 mm), number of teeth (32) etc.. Other specifications of gears are also obtained from ELCAM after giving pitch circle diameter and required numbers of teeth. The dedendum diameter is obtained as 42.18 mm, addendum diameter is obtained as 56.25 mm, base tangent length is obtained as 14.538 mm, face width is obtained as 4.9 mm and the number of teeth for span measurement is obtained as 2. Total 32 sets of experiments i.e. L_{16} orthogonal array were conducted by taking two teeth as one set, each at four different levels and at four different parameters. Single pitch deviation and MRR were calculated from these experiments. Later Optimization of parameters is done to get the best results.

3.1. Calculations of Single Pitch Error and MRR

MRR is a process in which undesired abundance material is expelled from a beginning work-part so the remaining part become closer to the desired shape. In Wire EDM, the material is removed by the spark discharges produced by the electric current. *Circular pitch* is defined as the distance between corresponding points of consecutive gear tooth measured along the pitch circle. *Single pitch error* is the difference between the theoretical circular pitch and actual measured values of a pitch for a given pair of teeth or the deviation between the actual measured pitch values between

any two adjacent tooth surfaces and the theoretical circular pitch.

Single pitch error (F_{pt}) = Theoretical Circular Pitch – Actual measured pitch values

Circular pitch can be calculated as

$$\text{Circular pitch } P = \frac{\pi}{P_d} \quad (1)$$

Where P_d is the Diametral Pitch and is calculated as the ratio of number of teeth to the Pitch circle diameter.

$$\text{Diametral Pitch } P_d = \frac{N}{D} \quad (2)$$

Where N is the number of teeth and D is the Pitch circle diameter in mm.

Theoretical circular pitch is given by the following formulae:

$$\text{Theoretical Circular Pitch } (F_p) = \frac{\pi}{P_d} = \pi \frac{D}{N} \quad (3)$$

Theoretical circular pitch or Theoretical F_{pt} value is constant in the experimentation after giving required numbers of teeth and pitch circle diameter. The actual F_{pt} is calculated by measuring the average of left flank (LF) and right flank (RF) of the gear using suitable software (Caliper pro 4.8).

Material Removal Rate (MRR) can be calculated by taking cutting speed (V_c), cutting length (L), time and material thickness into consideration.

Cutting speed (V_c) can be calculated as

$$V_c = 60 \frac{L}{t} \text{ m/min} \quad (4)$$

Where L is the cutting length in mm and t is the time in seconds

The Material removal rate (MRR) can be calculated by the following formula

$$MRR = V_c * h * k \text{ mm}^3/\text{min} \quad (5)$$

Where V_c is the cutting speed in m/min, h is the thickness of work-piece in mm and k is the diameter of workpiece in mm.

Multi-objective Optimization of Parameters

There are many techniques available for optimization. However in this study Taguchi Quality Loss function technique is used for optimization of response parameters. Taguchi method is an important tool in design of experiment method. Taguchi design is an orthogonal array method for designing the experimental procedure using different types of design like, two, three, four, five, and mixed level. In Taguchi, a loss function is developed from the error. Uncontrollable factors sometimes noise, causes error and results into loss. In WEDM, lower Pitch error and higher material removal rate are the indications of better performance. The user always tries to minimize the error and improve the material removal rate. So in the present research work the single pitch error is to be minimized and material removal rate is to be maximized. There are 16 sets of combinations conducted for the experiment out of which one will be the best combination out of the 16. So in order to find out the optimized result, Taguchi Quality Loss function technique is implemented.

Steps for calculating Taguchi Quality Loss function

According to the Taguchi Technique, the data's can be normalized in two ways.

- Lower the better (LB) function
- Higher the better (HB) function

The performance characteristics or output responses, whose

values are preferred as high, are calculated by using higher the better approach and the performance characteristics whose values are preferred as low, are calculated by using lower the better approach.

Step 1:

Considering the output responses:

For Lower the better (LB)

Quality loss function $L_{ij} = Y_{ij}^2$ (i.e. Square of the responses) (6)

For Higher the better (HB)

$$\text{Quality loss function } L_{ij} = 1/Y_{ij}^2 \quad (7)$$

Where Y_{ij} is the i^{th} performance of the response table in the i^{th} trial

Step 2: Calculation of Normalized Values

The data are normalized in order to avoid the effect of using different units and to reduce the variability. It is a transformation function performed to distribute the data evenly on a single input and to scale it into an acceptable range for further analysis. The normalized value always lies between 0 and 1.

The normalized function is given by the formula

$$N_{ij} = \frac{L_{ij}}{L^*} \quad (8)$$

Where $L^* = \max L_{ij}$

Step 3: Calculation of Total Loss function (T_{ij})

The average of the responses is considered for calculating T_{ij}

The total loss function or the Taguchi Loss function is given by the following formula

$$T_{ij} = \sum_{i=1}^n N_{ij} \quad (9)$$

Where n is the number of output responses.

Step 4:

Calculation of S/N ratio for T_{ij}

The S/N ratios are expressed on a decibel scale. The factor levels that have maximum S/N ratio are considered as optimal. The S/N ratio is used to determine the deviation of the performance characteristics from the desired value in Taguchi Quality loss method. The S/N ratio can be calculated as the logarithmic transformation of the loss function which is given by the following formulae:

$$N_j = -10 \log T_{ij} \quad (10)$$

Table 5 shows the multi objective optimization of response parameters by Taguchi Loss function.

TABLE V. MULTI OBJECTIVE OPTIMIZATION OF RESPONSE PARAMETERS USING TAGUCHI QUALITY LOSS

Sl no.	Normalization (N_{ij})		Taguchi Quality Loss (T_{ij})	S/N Ratio
	MRR	F_{pt}		
1	0.686	0.818	0.752	-2.47564
2	0.83	0.811	0.820	-1.71843
3	0.81	0.853	0.831	-1.60275
4	0.833	1	0.916	-0.75735
5	1	0.559	0.779	-2.16368
6	0.555	0.705	0.630	-4.01319
7	0.545	0.743	0.644	-3.82228
8	0.56	0.717	0.638	-3.89678
9	0.3	0.42	0.360	-8.87395
10	0.502	0.743	0.622	-4.11721
11	0.467	0.606	0.536	-5.40861
12	0.479	0.461	0.470	-6.55804
13	0.212	0.606	0.409	-7.76553
14	0.25	0.73	0.490	-6.19608
15	0.255	0.853	0.554	-5.12980
16	0.161	0.717	0.439	-7.15071

Table 6 presents the values of F_{pt} and MRR corresponding to sixteen sets of experiments. The results of the WEDM parameters in the single pitch error and MRR are presented graphically based on the experimental values obtained from table 6.

TABLE VI. INPUT PARAMETERS AND OUTPUT RESPONSES OBTAINED AT DIFFERENT RUNS

SI no.	Input Parameters				Actual F_{pt}			Theoretical F_{pt}	Single pitch error (F_{pt})	MRR
	T_{on}	T_{off}	W_f	W_t	LF	RF	Avg.			
1	110	50	3	6	8.81	8.77	8.79	9.81	1.02	1.91
2	110	52	4	7	8.60	8.66	8.63	9.81	1.18	1.74
3	110	54	5	8	8.51	8.70	8.60	9.81	1.21	1.76
4	110	56	6	9	8.70	8.66	8.68	9.81	1.13	1.73
5	112	50	4	8	8.76	8.90	8.83	9.81	0.98	1.58
6	112	52	3	9	8.73	8.69	8.71	9.81	1.10	2.13
7	112	54	6	6	8.72	8.64	8.68	9.81	1.13	2.15
8	112	56	5	7	8.67	8.73	8.70	9.81	1.11	2.12
9	114	50	5	9	8.93	8.99	8.96	9.81	0.85	2.89
10	114	52	6	8	8.68	8.68	8.68	9.81	1.13	2.24
11	114	54	3	7	8.56	9.03	8.79	9.81	1.02	2.32
12	114	56	4	6	8.86	8.98	8.92	9.81	0.89	2.29
13	116	50	6	7	8.78	8.78	8.78	9.81	1.02	3.43
14	116	52	5	6	8.68	8.70	8.69	9.81	1.12	3.17
15	116	54	4	9	8.59	8.60	8.59	9.81	1.21	3.14
16	116	56	3	8	8.66	8.73	8.69	9.81	1.11	3.94

It can be observed from Table 6 that in order to minimize single pitch error (LB) and maximize the MRR (HB) there exist an optimum values of pulse on time, pulse off time, wire feed rate and wire tension. In the present research work, from the Table 6, the multi objective output values obtained after conducting the experiments were single pitch error and MRR. Those two output responses were optimized and were combined by the above steps of Taguchi Quality Loss technique to obtain a single objective output function (Taguchi Quality Loss). Table 5 shows the step by step process of Taguchi Quality Loss optimization technique.

There are 16 combinational outputs obtained from software (Minitab 16) and the optimization is carried out for the best setting as shown in Table 5. For the 1st setting, the single pitch error and MRR obtained from the experiment is 1.02 and 1.91 respectively (Table 6). Single pitch error should be minimized and MRR should be maximized. So for minimization, lower the better should be considered and for maximization higher the better should be considered. For the 1st setting Y_{ij} for single pitch error is 1.02 and MRR is 1.91. Applying “(6)” and “(7)”, Quality loss function L_{ij} is calculated. L_{ij} for 1st set is $(1.02)^2=1.0404$ for single pitch error and $1/(1.91)^2=0.2741$ for MRR. In this way L_{ij} of all 16 combinations were calculated for single pitch error and MRR.

The maximum L_{ij} or L^* is assessed for both single pitch error and MRR from 16 combinations. Applying “(8)”, N_{ij} is calculated. N_{ij} for the 1st set is $1.0404/\text{maximum } L_{ij} = 0.818$ for single pitch error and $0.2741/\text{maximum } L_{ij} = 0.686$ for MRR.

Applying “(9)” Taguchi Quality Loss (TQL) is calculated by combining the two output functions to one. As there are two responses, so here n is 2. For the 1st set, TQL is calculated as $(0.686+0.818)/2=0.752$. In this way, TQL of all 16 combinations were calculated.

After calculating and obtaining all the responses, the regression equations are generated and objective functions are obtained. The objective function is obtained from the

MINITAB software by selecting the input responses (optimization variables) and output responses (constraints). The objective functions obtained for single pitch error, MRR and Taguchi Quality Loss functions are as follows.

Objective functions:

$$\text{MRR} = -28.37 + 0.2665 T_{on} + 0.0111 T_{off} - 0.0264 W_f + 0.0263 W_t$$

$$\text{Single Pitch Error} = 1.11 - 0.0084 T_{on} + 0.0144 T_{off} + 0.0127 W_f + 0.0122 W_t$$

$$\text{Taguchi Quality Loss (TQL)} = 7.18 - 0.0624 T_{on} + 0.0062 T_{off} + 0.01 W_f + 0.0145 W_t$$

IV. RESULTS AND DISCUSSION

4.1. Details of different observations

Fig. 3 shows the main effect plot diagram for Taguchi quality loss function after the outputs have been optimized. Higher the values in the graphs, better is the optimum results. It can be seen from fig. 3 that the highest values are at combinations 110-52-4-8, which indicates the best optimized setting of process parameters for cutting of the gears. However this combination is not present in the L16 combination. In order to find out the outputs of the obtained combination, a confirmatory test is required so that the required MRR and single pitch error can be evaluated at this setting. Fig. 4 shows the individual main effect plot for single pitch error and MRR. For data pre-processing in the Taguchi Quality Loss function, single pitch error is taken as ‘smaller the better’ and material removal rate is taken as the ‘larger the better’.

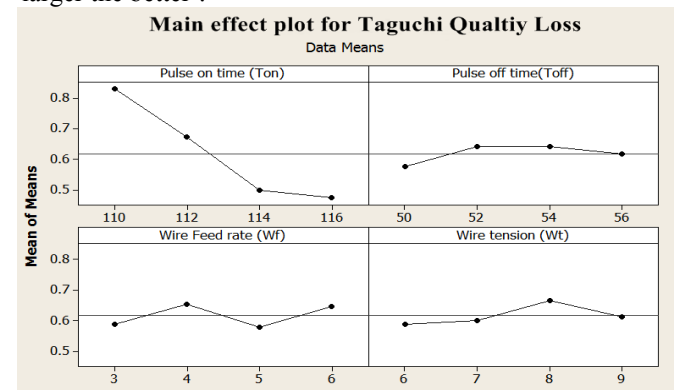


Fig. 3. Main effect plot diagram for Taguchi Quality Loss.

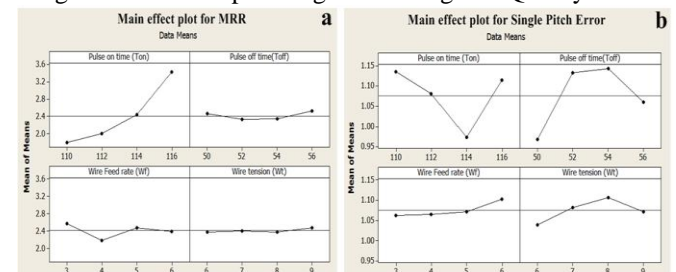


Fig. 4. Individual main effect plot diagram for (a) MRR and (b) single pitch error.

4.2. Confirmatory test

Confirmation test is done to find out the values of the optimized setting of the combinations obtained from the main effect plot which is not present in the Taguchi Loss function optimization table (Table 5). The optimal

combination of machining parameters has been determined in the previous analysis. Once the optimal level of the process parameters has been selected, it is the final step to predict and verify the improvement of the performance characteristic using that optimal level of the process parameters. The percentage change of Quality loss between predicted and experimental value for this optimal combination (T_{on} 1st level; 110, T_{off} 2nd level; 52, W_f 2nd level; 4 and W_t 3rd level; 8) is assessed from the main effect plot (Fig. 3). Again at this optimized setting the experiment was conducted and the experimental results were compared with the predicted ones. Table 7 compares the results of the confirmation experiments obtained by the predicted values and the experimental values of process parameters. As shown in table 7, the S/N ratio is improved from -1.800 to -4.180 (an improvement of 22.70%). In other words, the experimental results confirm the prior design and analysis for optimizing the machining parameters.

TABLE VII. RESULTS OF CONFIRMATORY TEST

Level	Optimal machining parameters	
	Prediction	Experiment
S/N ratio for Taguchi Quality Loss (TQL)	$T_{on1}T_{off2}W_{f2}W_{t3}$ -1.800	$T_{on1}T_{off2}W_{f2}W_{t3}$ -4.180

4.3. Effects of individual process parameter on responses

Effect of pulse off time: From Fig. 4 it is observed that single pitch error increases with the increase in pulse-off time but there is a decrease in MRR. It may be due to the fact that longer pulse-off time discharges more energy from the plasma channel which results in an increase in the sparking efficiency. This causes occurrence of the spark resulting in formation of irregular shaped craters which further results in higher values of single pitch error and low values of MRR.

Effect of pulse on time: It can be seen from Fig. 4 that with the increase in pulse on time, single pitch error initially decreases, attains a minimum value and then increases. Increase in the pulse-on time leads to increase in MRR as strong electric field at higher T_{on} facilitates the ionization of dielectric resulting in an increase in the period of transferring the discharge energy to the electrode which further results in rapid melting and evaporation of large amount of material. Higher values of T_{on} also results in an increase in discharge energy and cutting rate.

Effect of Wire Tension: Increase in the wire tension results in increase in both MRR and single pitch error. High water pressure and high induced reaction forces are the causes for the increase in both single pitch error and MRR.

Effect of Wire feed rate: At low wire feed rate, single pitch error is minimum and MRR is maximum. With the increase in W_f , single pitch error increases but in case of MRR, initially it decreases, increases to a certain point and again it decreases. This is because of the fact that the more discharge energy is being drawn by the wire per unit wire length at low wire feed rate. The spark concentration duration is reduced by the increased wire feed rate, thereby decreasing the wire-breakage which leads to low values of MRR and high values of single pitch error. With the increase in W_f , machining rate also increases.

4.4. ANOVA test

ANOVA test is used to find out the significant process parameters affecting the responses. If the P value (probability value) is less than 0.05, the factor is said to be significant. Table 8 shows the ANOVA test for Taguchi Quality loss. From the ANOVA table it is clear that pulse on time is the significant process parameter affecting the responses followed by pulse off time, wire feed rate and wire tension.

TABLE VIII. ANOVA TABLE FOR TAGUCHI QUALITY LOSS

Source	Degree of Freedom (DF)	Sequential sum of squares (Seq SS)	Adjusted sum of squares (Adj SS)	Adjusted mean square (Adj MS)	Fischer (F)	Probability (P)
T_{on}	3	0.334	0.334	0.111	10.10	0.045 (Significant)
T_{off}	3	0.011	0.011	0.003	0.35	0.793
W_f	3	0.018	0.018	0.006	0.56	0.679
W_t	3	0.014	0.014	0.004	0.44	0.741
Residual error	3	0.033	0.033	0.011		
Total	15	0.412				

V. MICROSCOPIC ANALYSIS

5.1. SEM image of machined workpiece

The section of the machined workpiece gear obtained at the optimized combination (T_{on} 110 T_{off} 52 W_f 4 W_t 8) was scanned under Scanning Electron Microscope (SEM) and different observations were made based on the analysis. Fig. 5 shows the typical SEM image of the work-piece material. From Fig. 5(a), some grains like structures were formed on the machined gear surface due to etching. The etchant used for this analysis is 50 ml distilled water and 50 ml nitric acid. The copper workpiece was dipped for 20 seconds into the etchant solution after the machining operation. The purpose of making the etchant solution is to analyse the grain boundaries and structures present on the copper workpiece after machining. Moreover some holes or voids were also found on the machined surface even if wire EDM provides good surface finish. This occurrence of holes might be due to the fluctuations in current and voltage resulting in the change of different amount of spark energy produced from the wire. Fig. 5(b) shows the top surface of the gear at 100X zoom.

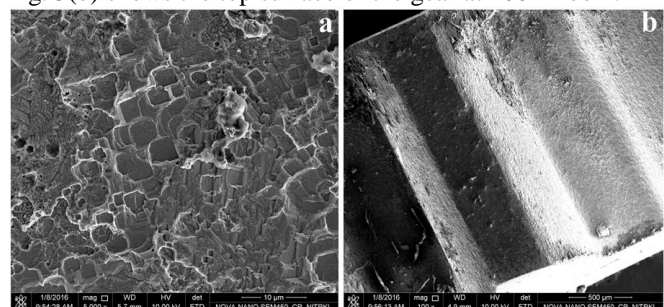


Fig. 5. SEM image of the workpiece material (a) grain like structures and (b) top surface of the gear at 100 X zoom. Similarly Fig. 6 shows the SEM image of the scanned workpiece at higher magnification zoom. It can be observed from Fig. 6(a) and Fig. 6(c) that the surface defects like heat affected zone (HAZ), bull eye and holes are found on the machined gear surface. Moreover there were formation of voids and craters at higher magnification zoom (10000 X). The formation of bull eye is due to the presence of oxygen

rich layer deposited due to the interaction of dielectric fluid. The formation of voids, craters, HAZ and holes are due to the decreased pulse on time and pulse off time at high wire tension resulting in an increase in the spark at low wire feed rate. Similarly from Fig. 6(b) and Fig. 6(d), surface craters, voids and debris are found on the scanned machined surface. The formation of debris is due to the rapid heating and cooling of the molten material or re-solidification of the molten material due to the spark produced from the wire. The formation of craters and voids is due to the solidification that melts at a high temperature produced from the spark due to low pulse on time.

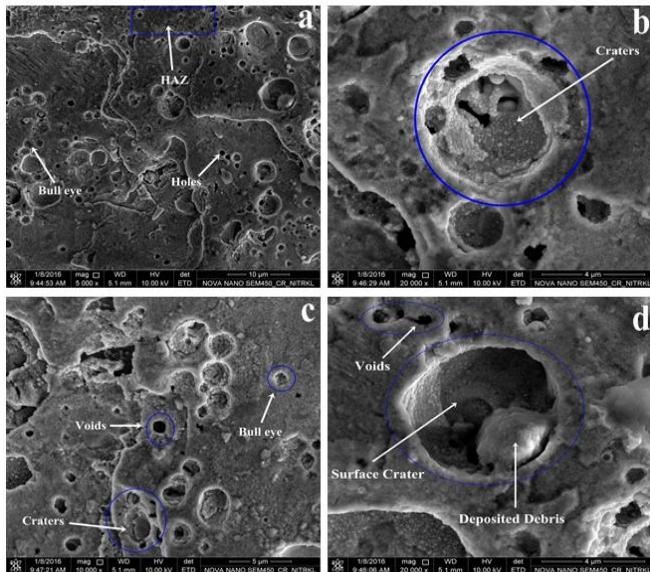


Fig. 6. Typical SEM image of the machined gear workpiece at higher magnification zoom.

5.2. SEM image of wire electrode

The section of the wire electrode machined to the workpiece at the optimized combination ($T_{on} 110T_{off} 52 W_f 4 W_t 8$) was scanned under Scanning Electron Microscope (SEM) and different observations were made based on the microstructural analysis. Fig. 7 shows the SEM image of wire electrode after the machining of gear operation. Fig. 7(a) and Fig. 7(c) shows that the wire suffers craters, cracks and wire wear after the machining operation. As the wire approaches towards the workpiece, the sparks produced from the wire creates rupture. Due to the higher wire tension, the wire remains straightened between the upper and lower guides and as the wire moves at a lower feed rate ($W_f=4$), the time spent to machine the workpiece increases thereby causing cracks, craters and maximum wire wear from the electrode surface as well as workpiece surface. It can be also observed from the Fig. 7(b) and Fig. 7(d) that a discoloured black layer is formed along with the micro voids, surface cracks, craters and micro globules on the electrode surface after machining. The discoloured black layer is formed due to the spark at a particular region over a period of time at low wire feed rate and low pulse off time. Micro voids, surface cracks and craters are due to the high sparks produced due to low pulse on time at high servo voltage.

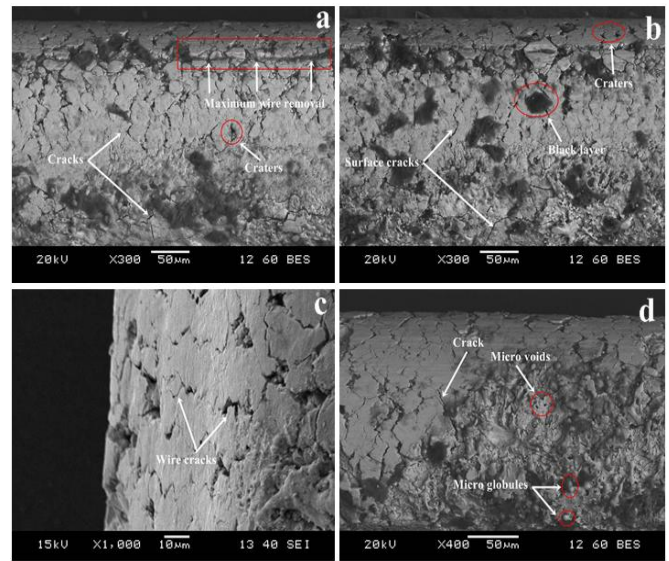


Fig. 7. SEM image of wire electrode after machining.

5.3. XRD analysis

X-Ray Diffraction Spectrometer is the most sophisticated and powerful analytical tool available for identifying unknown crystalline substances present in the material. When X-ray is directed to a crystal, the atom of each crystal gets interacted with the X-ray by exciting their electrons, causing them to vibrate with the frequencies of the incoming radiation. Bragg's law: $n\lambda = 2d \sin\theta$ explains the relationship between angle of the diffraction peaks (2θ) and the inter-atomic spacing (d-spacing) of a crystalline lattice. XRD is mostly done to know the shape and size of the unit cell for any compound. In the present paper, XRD analysis is done to know the chemical composition on the material surface after it is being machined by brass wire. Fig. 8 shows the XRD diffractograms at 2θ ranging from 10° to 90° of machined gear surface at optimized setting ($T_{on} 110T_{off} 52 W_f 4 W_t 8$) of the response. The wire is in contact to the copper workpiece. Copper Molybdenum chloride, Ferrocenylcopper and Copper Nickel compounds were formed after the XRD analysis. The presence of Molybdenum and Nickel compound might be due to the deposition of foreign elements present in the dielectric fluid. As the dielectric fluid is recycled and reused, the external compounds might have been carried away by the dielectric and gets deposited on the workpiece. The leftover particles of previously machined elements might have been flushed away by the dielectric and flows to the water tank. As the same water is recycled, the external elements might have been deposited over the workpiece material by the action of rapid heating and cooling of the spark. From Fig. 8 it is observed that the highest peak is located at $2\theta 16.831^\circ$, d spacing 5.272\AA , followed by $2\theta 13.960^\circ$, d spacing 6.349\AA and $2\theta 74.887^\circ$, d spacing 1.267\AA . Copper Molybdenum chloride is located at the highest peak where as Copper Nickel is located at lower peak of d-spacing 1.267\AA .

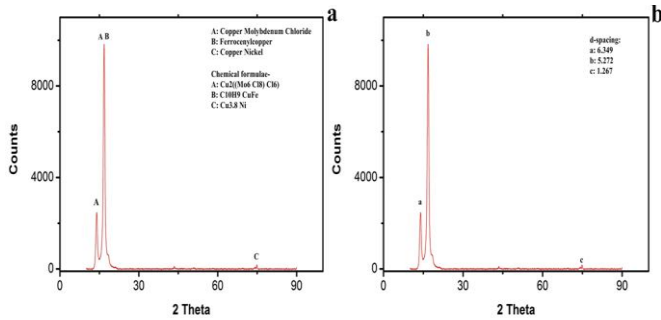


Fig. 8.XRD diffractograms at 2θ ranging from 10⁰ to 90⁰ of machined gear surface at optimized setting of the response.

VI. NUMERICAL MODELLING OF WORKPIECE

ANSYS® is one of the most powerful and flexible tool for steady state thermal analysis of both 2D and 3D structures. In this analysis, steps like engineering data, geometry, model, Set up, meshing, boundary conditions and solution are available in the ANSYS workbench. The analysis like temperature, total heat flux etc. can be analysed from thermal analysis whereas equivalent stress, strain etc. can be analysed from static structural analysis. The whole analysis is carried out for the workpiece material only neglecting the wire part. The thermal properties of the workpiece material (copper) are extracted from the general material property database (engineering data) of ANSYS workbench. The thermal conductivity of copper is taken as 400 W/mk and density is taken as 8.9 g/cm³. The geometry is modelled by giving the dimensions of the workpiece. The purpose of modelling is to analyse the maximum temperature of the workpiece material attained during machining.

6.1. Model creation

The model is created and generated from the geometry data base considering the length, width and thickness of the workpiece to be 10 mm, 5 mm and 3 mm respectively. The next step is to select meshing for the material. Meshing is important as it divides the elements into smaller parts so that the exact solution can be attained considering each element and nodes of the workpiece model. The smaller mesh element size gives more accurate results during the analysis. Number of elements size (18790) and nodes (86353) were extracted from the model after giving automated type of meshing. Fig. 9(a) and Fig. 9(b) shows the geometry model creation and meshing applied to the model in ANSYS workbench.

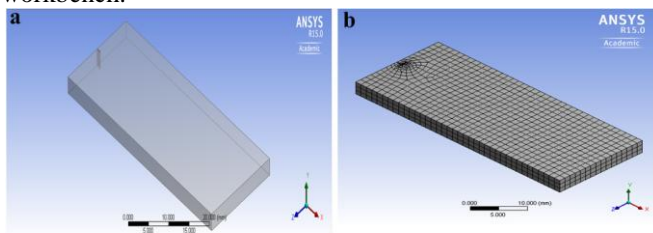


Fig. 9.(a) Geometry model creation and (b) meshing of the workpiece using ANSYS workbench.

Some assumptions must be followed while considering the model such as the model is developed for single spark only,

the workpiece should be free from all types of stresses, the work domain is considered as asymmetric and the material properties of the workpiece is temperature dependent.

6.2. Applying boundary conditions

Once the geometry is created with proper meshing, certain boundary conditions must be applied to the model. The material is fixed at one end while the other remains unfixed. The gap between the wire and the work piece is filled with water from top to bottom. The heat flux “(1)” i.e. 4e-3 W/mm² and convective heat transfer coefficient (free convection of air at temperature 30°C is 4e-4 W/m²K) were applied to the model as the boundary conditions. The total heat flux Q_w is given by the following formula [13]:

$$Q_w = \frac{4.45PVI}{\pi R^2} e^{-4.5 \left[\left(\frac{k}{R^2} \right) \right]} \quad (11)$$

Where P is the energy distribution coefficient (constant = 0.38) as studied by Kunieda and Furudate [14], I is the peak current, V is the voltage between anode and cathode, R is the spark radius and k is the wire radius.

The sparks generated in the wire is assumed to be single spark. The equation for the spark radius (μm) is given by the formulae [15]:

$$R = 2.04e^{-3} I^{0.43} T_{on}^{0.44} \quad (12)$$

Where, T_{on} is the Pulse on time and I is the peak current. Table 9 shows the values of parameters considered in modeling the workpiece. Similarly Fig. 10 displays the boundary condition applied to the model.

TABLE IX. PARAMETER VALUES USED IN THE MODELLING OF WORKPIECE

Parameters	Units	Values (Optimized Setting)
		Brass electrode $T_{on} 14 T_{off} 46 W_f 7$ $S_p 55$
Energy distribution coefficient (P)		0.38
Current (I)	A	1
Servo Voltage (V)	V	55
Spark radius (R)	mm	0.000324
Thickness of the workpiece (h)	mm	3
Radius of the wire (k)	mm	0.125

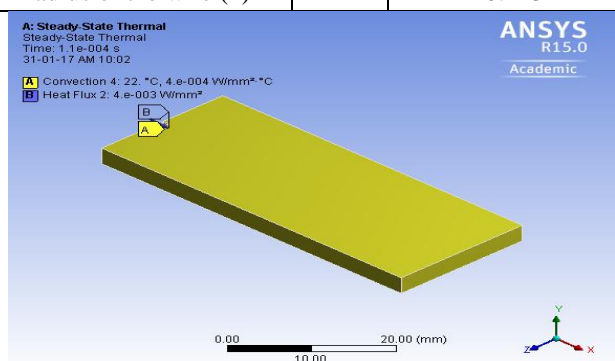


Fig. 10.Boundary conditions applied to the model.

6.3. Solutions and results

The solutions were obtained after the boundary conditions have been applied to the model. Fig. 11 displays the temperature obtained for the workpiece material in steady state thermal analysis. From Fig. 11 it is concluded that the maximum temperature of the material obtained from the steady state thermal model machined by brass wire electrode is 22.87 °C whereas the minimum temperature of the material obtained was 22 °C. The maximum temperature of the material is produced near to the sparking region of the wire. As the work-piece is in contact to the dielectric fluid the dielectric medium cools down the body temperature of the material, allowing the workpiece to obtain a temperature less than the room temperature.

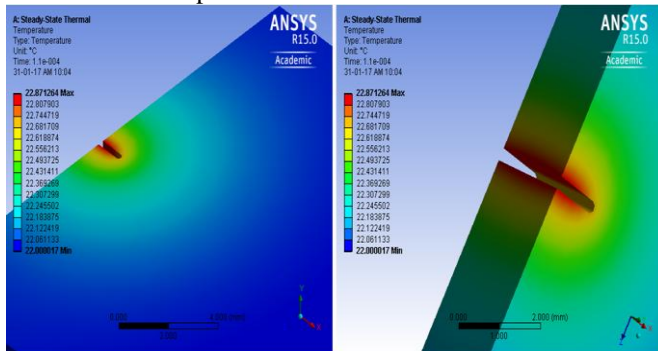


Fig. 11. Temperature distribution of the workpiece obtained in steady state thermal analysis.

VII. CONCLUSIONS

The gear profile was obtained by machining the spur gear by Wire EDM. The error in the gear was investigated and following conclusions were made based on the experimental work and results obtained.

- The gear profile is obtained by minimizing the deviations in the single pitch error and maximizing the MRR. It can be observed that to minimize single pitch error and maximize the MRR there exist an optimum values of pulse on time, pulse off time, wire feed rate and wire tension.
- The output responses are combined and a single response (Taguchi Quality Loss) is obtained by optimizing the response parameters. ANOVA test confirms that the input parameters i.e. pulse on time is found to be highly significant factor affecting the responses followed by pulse off time, wire feed rate and wire tension.
- Considering the individual effects of output responses, pulse on time and wire tension is the determining factor in affecting the single pitch error and MRR. With the increase in the pulse on time and wire tension, single pitch error and MRR also increases.
- The error in the gear is mainly due to the fluctuations in the voltage and current which leads to the increase in the spark discharge energy which further results in increase in the cutting speed, resulting in the uneven surface distribution.
- The confirmations test shows that the S/N ratio is

improved from -1.800 to -4.180 (an improvement of 22.70%), which confirm the prior design and analysis for optimizing the machining parameters.

- Microstructural analysis has been carried out for both workpiece and wire at the optimized setting of the response. The surface defects like craters, voids, holes etc. were formed on the gear cut machined surface due to high temperature and high spark energy density produced from the wire. Similarly wire cracks, craters and wire wear can be identified on the wire electrode surface due to the increased energy of the spark at low pulse on time and high servo voltage.
- XRD analysis was implemented to know the deposition of foreign particles or external elements migrated to the workpiece material. It has been analyzed that the elements like Copper Molybdenum chloride, Ferrocenylcopper and Copper Nickel compounds were deposited on the material surface due to the recycling of the dielectric fluid.
- Numerical modeling of workpiece has been carried out to know the mechanics involved in the process. It has been found that the maximum temperature of the workpiece material after it has been machined by brass wire was found to be 22.87 °C.
- The optimized setting obtained for the copper gear material machined by brass wire electrode can be further used in machining of other spur gears to produce high quality meso gears.

REFERENCES

[1] J. Pradhan, S. Guha, and B.B. Pradhan, "Review on process parametric optimization of wire electric discharge machining{ /ArticleTitle PT}," Int. J. Des. Manu. Technol.,{PT Year}vol. 11{/Volume PT}({PT Issue}1{/Issue PT}), pp. 1-7{/PageRange PT}, 2017.

[2] {PT Authors}T.A. Spedding, and Z.Q. Wang. {PT ArticleTitle}"Study on modeling of wire EDM process{/ArticleTitle PT},"J. Mater. Proces. Technol.,{PT Year}vol. {PT Volume}69{/Volume PT}, pp. 18-28{/PageRange PT}, 1997.

[3] {PT Authors}A.W.J. Hsue, and H.C. Su,{PT ArticleTitle}"Removal analysis of WEDM tapering process and its application to generation of precise conjugate surface{/ArticleTitle PT},"J. Mater. Proces. Technol.,{/JournalTitle PT}vol. {PT Volume}149{/Volume PT}({PT Issue}1-3{/Issue PT}), pp. 117-123{/PageRange PT}, 2004.

[4] {PT Authors}D. Rakwal, E. Bamberg, and E{/Authors PT}. {PT ArticleTitle}Slicing, "Cleaning and kerf analysis of germanium wafers machined by wire electrical discharge machining{/ArticleTitle PT},"J. Mater. Proces. Technol.,{/JournalTitle PT}vol. {PT Volume}209{/Volume PT}({PT Issue}8{/Issue PT}), pp. 3740-3751{/PageRange PT}, 2009.

[5] {PT Authors}D. Scott, S. Bovina, and K.P.

- Rajurkar, {PT ArticleTitle}“Analysis and optimization of parameter combinations in wire electrical discharge machining{/ArticleTitle PT},”*Int.J. Prod. Res.*, {PT Year} vol. {PT Volume}29{/Volume PT}({PT Issue}11{/Issue PT}), pp. 2189-2207{/PageRange PT}, 1991.
- [6] {PT Authors}Y.S. Tarng, S.C. Ma, and L.K. Chung, {PT ArticleTitle}“Determination of optimal cutting parameters in wire electrical discharge machining{/ArticleTitle PT},”*Int. J. Mach. Tool. Manuf.*, {PT Year} vol. {PT Volume}35{/Volume PT}({PT Issue}12{/Issue PT}), pp. 1670-1693{/PageRange PT}, 1995.
- [7] {PT Authors}Y.S. Liao, J.T. Huang, and H.C. Su, {PT ArticleTitle}“A study on the machining parameters optimization of the wire electrical discharge machining{/ArticleTitle PT},”*J. Mater. Proces. Technol{/JournalTitle PT}*., vol. {PT Volume}71{/Volume PT}, pp. 487-493{/PageRange PT}, 1997.
- [8] {PT Authors}J.T. Huang, and Y.S. Liao, {PT ArticleTitle}“Optimization of machining parameters of Wire-EDM based on grey relational and statistical analyses{/ArticleTitle PT},”*Int.J. Prod. Res{/JournalTitle PT}*., vol. {PT Volume}41{/Volume PT}({PT Issue}8{/Issue PT}), pp. 1707-1720{/PageRange PT}, 2003.
- [9] {PT Authors}R. Ramakrishnan, and L. Karunamoorthy, “Multi response optimization of Wire EDM operations using robust design of experiments{/ArticleTitle PT},”*Int. J. Adv. Manuf. Technol.*, {PT Year} vol. {PT Volume}29{/Volume PT}, pp. 105-112{/PageRange PT}, 2006.
- [10] {PT Authors}K. Kanlayasiri, and P. Jattakul, {PT ArticleTitle}“Simultaneous optimization of dimensional accuracy and surface roughness for finishing cut of wire-EDMed K460 tool steel{/ArticleTitle PT},”*Prec. Eng.*, {PT Year} vol. {PT Volume}37{/Volume PT}, pp. 556-561{/PageRange PT}, 2013.
- [11] {PT Authors}K. Gupta, and N.K. Jain, {PT ArticleTitle}“On micro-geometry of miniature gears manufactured by WEDM{/ArticleTitle PT},” {PT JournalTitle} *Mater.Manuf. Process.*, vol. {PT Year} {PT Volume}28{/Volume PT}({PT Issue}10{/Issue PT}), pp. 1153-1159{/PageRange PT}, 2013.
- [12] {PT Authors}N. Tosun, C. Cogun, and G. Tosun, {PT ArticleTitle}“A study on kerf and material removal rate in wire electrical discharge machining based on Taguchi method{/ArticleTitle PT},”*J. Mater. Proces. Technol{/JournalTitle PT}*., {PT Year} vol. {PT Volume}152{/Volume PT}({PT Issue}3{/Issue PT}), pp. 316-322{/PageRange PT}, 2004.
- [13] S.N. Joshi, and S.S. Pande, {PT ArticleTitle}“Thermo-physical modeling of die-sinking EDM process{/ArticleTitle PT},”*J. Manuf.Proces.*, vol. {PT Volume}12{/Volume PT}({PT Issue}1{/Issue PT}), pp. 45-56{/PageRange PT}, 2010.
- [14] K. Kuneida, and C. Furudate, “High precision finish cutting by dry WEDM{/ArticleTitle PT},”*J. Mater. Proces. Technol{/JournalTitle PT}*., vol. 149, pp. 77-82, 2001.
- [15] R. Rajendran, and M.S.P. Vendan, “Study of workpiece thermal profile in electric discharge machining{/ArticleTitle PT},” {PT JournalTitle} *Int. J. Eng. Res. Technol.*, vol. 3(1), pp. 3498-3503, 2014.